Contrib Mineral Petrol (2005) 149: 527–540
DOI 10.1007/s00410-005-0666-7

ORIGINAL PAPER

Daisuke Takagi · Hiroaki Sato · Mitsuhiro Nakagawa

Experimental study of a low-alkali tholeiite at 1–5 kbar: optimal condition for the crystallization of high-An plagioclase in hydrous arc tholeiite

Received: 25 February 2003 / Accepted: 1 March 2005 / Published online: 13 May 2005

Abstract We conducted melting experiments on a low-alkali tholeiite (SiO_2 ~52 wt%, MgO ~6.5 wt%, CaO/Na_2O~4.4, Al_2O_3/SiO_2 ~0.33) under both H_2O-undersaturated and H_2O-saturated conditions to investigate the effect of H_2O on the Ca–Na partitioning between plagioclase and melt. Experiments were performed in the temperature and pressure ranges of 1,000–1,300°C and 1–5 kbar, respectively, with varying H_2O contents of 0–12wt%. Redox condition was 0–2 log unit above NNO (nickel–nickel oxide) buffer. Temperature-bulk H_2O diagrams for the low-alkali tholeiite are constructed at 1, 2, and 5 kbar, and compositions of near-liquidus plagioclase and coexisting melt are determined. To exclude the effect of melt composition (CaO/Na_2O and Al_2O_3/SiO_2 ratios) on plagioclase composition and to reveal the effect of H_2O on An ($=100\times Ca/(Ca+Na)$) content and K_D^{Ca-Na} ($=(Ca/Na)_{pl}/(Ca/Na)_{melt}$), we focused on the composition of near-liquidus plagioclases which crystallized from melts with nearly constant CaO/Na_2O and Al_2O_3/SiO_2 ratios. Our experimental results show that, at each experimental pressure, An content of the near-liquidus plagioclase and the K_D^{Ca-Na} almost linearly increases as H_2O content in melt increases. Each of the An content and the K_D^{Ca-Na} variations in a low-alkali tholeiitic system (CaO/Na_2O~4.0–4.5, Al_2O_3/SiO_2 ~0.27–0.33) can be described by one equation using temperature, pressure, and melt H_2O content as parameters. An content and K_D^{Ca-Na} of liquidus plagioclase increases with increasing melt H_2O and with decreasing pressure, elucidating that nearly H_2O-saturated conditions of 2–3 kbar is optimal for the crystallization of the most An-rich plagioclase ($>An_{88}$). We suggest this pressure condition of 2–3 kbar, corresponding to depth of 7–11 km, plays an important role for the origin of An-rich plagioclase in H_2O-rich low-alkali tholeiite. At pressures more than ca. 4 kbar, crystallization of liquidus Ca-rich clinopyroxene decreases the CaO/Na_2O ratio of liquid, thus prohibiting the crystallization of high-An plagioclase from hydrous tholeiite.

Editorial responsibility: T.L. Grove

D. Takagi
Graduate School of Science and Technology, Kobe University, Nada-ku Kobe, 657-8501, Japan

H. Sato (✉)
Department of Earth and Planetary Sciences, Kobe University, Nada-ku Kobe, 657-8501, Japan
E-mail: hsato@kobe-u.ac.jp

M. Nakagawa
Department of Earth and Planetary Sciences, Hokkaido University, Kita-ku Sapporo, 060-0810, Japan

Present address: Sanbonmatsu High School, Sanbonmatsu Higashi-Kagawa, 769-2601, Japan

Introduction

Extremely An-rich plagioclases ($>An_{90}$) are commonly observed in arc basalts ejected at volcanic fronts (e.g. Kimata et al. 1995). Because the origin is expected to provide an important constraint on island arc magmatism, many petrological and experimental studies have been carried out. Early studies suggested that such an An-rich plagioclase could crystallize from melts with high H_2O content (e.g. Arculus and Wills 1980), or unusually high CaO/Na_2O ratio (e.g. Duncan and Green 1987), or high Al_2O_3 content (Beard and Borgia 1989). Sisson and Grove (1993a) determined K_D^{Ca-Na} ($=(Ca/Na)_{pl}/(Ca/Na)_{melt}$) ~1.7 at 2 wt% H_2O, ~3.4 at 4 wt% H_2O, and ~5.5 at 6 wt% H_2O in high-alumina basalt (HAB) compositions, and concluded that such An-rich plagioclases in HAB grew from melts with high H_2O contents up to 6 wt%. Furthermore, high H_2O concentrations in HABs were confirmed by direct measurement of glass inclusion in olivine phenocrysts (Sisson and Layne 1993). Panjasawatwong et al. (1995) suggested that extremely depleted parental magmas ($CaO/Na_2O>8$) with low H_2O contents (1–3 wt%) are required for the crystallization of such An-rich plagioclase.

To discuss the chemical and physical conditions at which An-rich plagioclase crystallized, it is important to evaluate each of the effect of melt composition, temperature, and pressure on plagioclase-melt equilibria. Previous experimental studies have demonstrated that melt CaO/Na_2O and Al_2O_3/SiO_2 ratios, H_2O content, temperature, and pressure are parameters affecting An content of liquidus plagioclase (Housh and Luhr 1991; Sisson and Grove 1993a; Longhi et al. 1993; Panjasawatwong et al. 1995), although these studies included variable melt compositions, H_2O contents, temperatures and pressures, and did not intend to evaluate the effect of one of the parameters on the An content and K_D^{Ca-Na} keeping other parameters constant. In the present study, to exclude the effect of melt composition on plagioclase composition and to reveal the effect of H_2O on An content and K_D^{Ca-Na}, we focus on the compositions of near-liquidus plagioclases which crystallized from nearly constant melt composition (CaO/Na_2O and Al_2O_3/SiO_2 ratios).

Experimental methods

Starting materials

Two starting materials were prepared for the experiments. One is whole-rock powder of a low-alkali tholeiite (sample IWL16) ejected from Iwate volcano, which is a representative Quaternary volcano located in the volcanic front of NE Japan (Nakagawa 1987; Onuma 1962). The sample was selected as representing the highest Mg# (Mg/(Mg + Fe) = 0.55) low-alkali tholeiite of the last eruption (A.D. 1732) of Iwate volcano. The rock contains ca. 1 vol% of olivine (Fo_{74-85}), 25 vol% of plagioclase (mainly An_{85-94}, MgO < 0.2 wt%, FeO* < 0.9 wt%), 2 vol% of augite (Mg# ~70–85), and 7 vol% of orthopyroxene (Mg# ~70–81) as phenocrysts. Maximum An content of the plagioclase phenocrysts is $An_{93.5}$. The whole-rock powder was prepared by crushing with a hammer (pure iron on iron plate) and then pulverized by agate mortar for ca. 1 h. The other is the glass powder made by melting IWL16 at 1,500°C in a one-atmosphere furnace in air for 5 h, and subsequently pulverized. The bulk chemical compositions of the starting materials were obtained by X-ray fluorescence analysis and presented in Table 1. The tholeiite is characterized by intermediate CaO/Na_2O ratio (4.3–4.4) and Al_2O_3/SiO_2 ratio (0.32–0.34) (Fig. 1).

Table 1 Compositions of starting materials

	Yakehashiri lava (IWL16)	
	Whole-rock	Glass
[Wt%[a]]		
SiO_2	53.09	52.00
TiO_2	0.77	0.74
Al_2O_3	16.88	17.45
Fe_2O_3[b]	10.43	10.94
MnO	0.18	0.17
MgO	6.53	6.50
CaO	9.61	9.72
Na_2O	2.22	2.18
K_2O	0.22	0.21
P_2O_5	0.08	0.08
CaO/Na_2O	4.33	4.45
Al_2O_3/SiO_2	0.32	0.34

[a] XRF analyses, recalculate to 100%
[b] Total Fe as Fe_2O_3

Equipments and run charges

Experiments at 1–2 kbar

The experiments (1–2 kbar) were carried out using the internally heated pressure vessel (IHPV) of KOBELCO installed at Kobe University. The apparatus uses argon as pressurizing medium and attains a maximum pressure of 2 kbar. Pressure is monitored by Heise gauge and maintained to ca. 3% of the nominal values. The experimental charges were placed near the tip of thermocouples, where a homogeneous temperature was maintained. The lower part of the vessel is at low temperature enough to quench the charges (< 300°C; Sato et al. 1999). After each run, the charges were dropped to

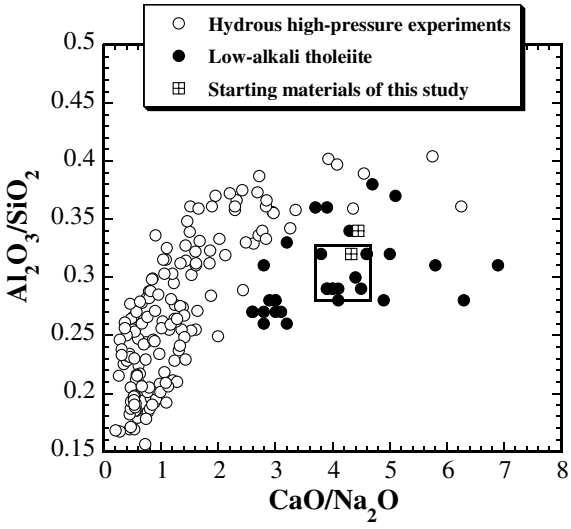

Fig. 1 Plots of CaO/Na_2O vs. Al_2O_3/SiO_2 weight ratios of plagioclase saturated melts obtained by hydrous experiments from literatures (*open circle*), bulk compositions of aphyric low-alkali tholeiitic basalt (*solid circle*), and starting materials in our experiments (*crossed square*). Compositional range of melt coexisting with near-liquidus plagioclase obtained in this study is also shown as *large open square*. Data sources for hydrous experiments; Baker and Eggler (1987), Housh and Luhr (1991), Sisson and Grove (1993a, 1993b), Panjasawatwong et al. (1995), Metrich and Rutherford (1998), Moore and Carmichael (1998), Martel et al. (1999), and Scailet and Evans (1999). Data sources for low-alkali tholeiitic basalts; Fiji arc (Gill and Whelan 1989), Mariana arc (Bloomer et al. 1989), Kurile arc (Avdeiko et al. 1991) and Izu-Ogasawara arc (Tsukui and Hoshino 2002; A-Miyasaka and Nakagawa 2002). Note that hydrous experiments on low-alkali tholeiitic composition have been sparsely carried out

the cooler part of the vessel by electrically cutting the molybdenum wire hanging the charge, and quenched. Experimental temperature was measured with a W-Re5/26 thermocouple positioned in the hottest part of the pressure vessel, and controlled by an automatic regulator. Temperature at the sample site was calibrated against melting point of copper and gold at the pressure (Mirwald and Kennedy 1979). Uncertainties on temperature determinations are ±5°C.

The experimental charges were prepared as follows. The double capsule method was used to buffer oxygen fugacity with solid Ni-NiO (9 : 1) assemblage. A tube (2–3/2.0 mmϕ1and 1.4 cm long), which consists of metal material (Pt, $Ag_{70}Pd_{30}$, $Ag_{50}Pd_{50}$, $Au_{70}Pd_{30}$, and $Au_{75}Pd_{25}$), was welded on one end and weighed. Distilled water was injected with a micro syringe and the capsule was weighed. Then, ca. 30 mg of powder starting material was inserted and weighed, and then welded shut on the other end and weighed. The weight loss during welding was very small (generally <0.00003 g) compared with the amount of water added. The sealed capsule was kept at 120°C in an oven for several tens of minutes, and reweighed to ensure good sealing of the capsule (leak check). Prepared sample capsule was put into the outer capsule (Au, Pt; 5.0/4.7 mmϕ1and 4.0 cm long) with distilled water and Pt capsule (3.0/2.7 mmϕ 1and 2.0 cm long) which contains distilled water and powder of Ni-NiO and was not welded but only shut. And then, the outer capsule was welded, weighed and leak checked again. Only capsules that did not leak were run at elevated pressure and temperature. The double capsule method we used is slightly different from that of Sisson and Grove (1993a) in the point that the latter authors did not weld shut the inner sample capsule, which facilitated more effective buffering of the system.

Following quenching, the experimental charges were weighted to measure volatile loss and punctured to verify the presence of water. The double capsules, which verified the presence of water, were opened, and sample capsules and buffer capsule were taken from the charges. Buffer capsule were prepared for buffer check and sample capsules, which were considered successful, were mounted in epoxy resin, polished on one side, and analyzed by electron microprobe.

Experiments at 5 kbar

The experiments (at 5 kbar) were carried out using a solid media 0.5-inch piston cylinder apparatus installed at Kobe University. Talc-Pyrex outer sleeves and fired pyrophyllite inner sleeves with graphite heater were used in the furnace assembly. The hot piston-out method was employed. Temperature was measured and controlled with $Pt/PtRh_{13}$ thermocouples without correction for the effect of pressure on the emf. Temperature at the sample site was calibrated against melting point of copper at pressure (Mirwald and Kennedy 1979). Temperature gradient within the furnace assembly was determined by repeatedly using two thermocouples and the results show the gradient was <30°C/sample capsule (ca. 8 mm). Accuracy in the temperature determination is believed to be in ±10°C. Pressure correction was also conducted against the melting point of NaCl at 5 kbar (Akella et al. 1969) and quartz-coesite phase boundary (T. Kawasaki, personal communication), and 17.5% correction for friction was applied. Uncertainty in the pressure determination is considered to be ±5% near 5 kbar.

Starting materials (ca. 10 mg) with desired water contents were sealed in an $Au_{75}Pd_{25}$ sample capsule (2.3/2.0 mmϕ1 and 8 mm long) to avoid Fe loss to sample container (Kawamoto and Hirose 1994). The method to make sample capsule is the same as that described in the previous section. Runs were quenched at run pressure by cutting the power to the furnace, and then the run charge was opened and the sample capsule was mounted in epoxy resin, polished on one side, and analyzed by electron microprobe.

Run procedures

Three experimental procedures were employed, (1) *melting experiments with the whole-rock powder as starting material*, (2) *crystallization experiments with the whole-rock powder as starting material, and* (3) *crystallization experiments with the glass as starting material*. In the experiments of (1) and (3), 1–2 charges were heated and held at a constant temperature for a prescribed period. In the experiments of (2), charges were firstly heated to a higher temperature (above 20–50°C of the run temperature) for 0.5–1 h, and then cooled down to the run temperature in ca. 1 min, and kept at that temperature for a prescribed period. Experimental durations varied between 17 h to 65 h, generally decreasing with increasing temperature to approach equilibration (Table 2).

All experiments at 1 and 5 kbars were carried out following the run procedure (3). However, in the early stage of this study (experiments at 2 kbar), run procedures of (1) and (2) were also performed. In microprobe analyses for run products obtained by the procedure (1), it is difficult to distinguish between the newly crystallized phase and the relict crystals. Therefore, the run products given by the procedure (1) were only used to determine phase stabilities, whereas the phase compositions were not used for discussions below. Run products given by the procedure (2) and (3) were mainly used for discussions below.

Analytical methods

Electron microprobe analyses were performed with JEOL JXA-8900 at the Venture Business Laboratory of Kobe University, under 15 kV acceleration voltage and 12 nA sample current using ZAF correction. Counting time of 20 s (10 s for Na_2O) with a focused beam was

Table 2 Experimental conditions and results of selected runs

Charge#	Starting material[a]	Capsule	H_2O in[b] (wt%)	Run procedure[c]	T (°C)	Duration (h)	Phases[d]	H_2O melt (wt%)[e]	H_2O by difference[f]	$K_{D_{Ol-melt}}^{Fetot-Mg}$	Δ NNO[g]	$\Sigma R^{2\,h}$	ΔFeO (%)[i]
1 kbar													
# 133	Glass	$Au_{75}Pd_{25}$	0.3	3	1200	18.5	gl(98), pl(2)	0.3	0.7	-	-	3.28	−16.6
# 129	Glass	$Ag_{50}Pd_{50}$	2.0	3	1150	20	gl(95), ol(1), pl(4)	2.1	2.4	0.23	+1.3/+0.5*	0.50	−6.4
# 148	Glass	$Ag_{50}Pd_{50}$	2.8	3	1100	25.5	gl(80), ol(4), pl(13), mt(3)	*3.3*	2.9	0.20	+1.3/+1.6*	0.09	0.2
# 149	Glass	$Ag_{50}Pd_{50}$	5.1	3	1100	25.5	gl(88), ol(3), pl(6), mt(3)	*3.3*	3.7	0.20	+1.8/+1.6*	0.08	0.2
2 kbar													
# 103	Glass	$Ag_{50}Pd_{50}$	1.0	3	1150	21	gl(96), pl(4)	1.0	1.8	-	-	0.16	−1.0
# 107	Glass	$Ag_{50}Pd_{50}$	1.5	3	1150	21	gl(100), pl(tr)	1.5	1.6	-	-	0.27	−2.1
# 66	WR-powder	$Ag_{70}Pd_{30}$	2.7	2	1130/1100	1/22	gl(98), pl(2)	2.8	4.1	-	-	1.68	−11.7
# 109	Glass	$Ag_{50}Pd_{50}$	2.9	3	1100	27	gl(94), ol(1), pl(3), mt(2)	3.1	4.5	0.23	+1.3/+0.7*	0.04	0.0
# 116	Glass	$Ag_{70}Pd_{30}$	3.9	3	1050	35	gl(93), ol(3), pl(2), mt(2)	4.2	6.7	0.24	+1.6/−0.1*	0.07	−0.2
# 64	WR-powder	$Ag_{70}Pd_{30}$	4.3	2	1050/1030	1/32	gl(67), ol(4), pl(16), cpx(6), opx(2), mt(5)	*4.9*	4.5	0.25	+0.9/−0.7*	0.39	−0.2
5 kbar													
# P4	Glass	$Au_{75}Pd_{25}$	0.0	3	1250	25	gl(91), pl(9)	0.0	1.6	-	-	0.20	−2.9
# P15	Glass	$Au_{75}Pd_{25}$	1.6	3	1180	30	gl(75), pl(17), opx(5), mt(3)	2.1	2.8	-	-	0.03	0.3
# P9	Glass	$Au_{75}Pd_{25}$	3.0	3	1150	29.5	gl(85), pl(8), opx(2), mt(5)	3.5	3.7	-	-	0.01	−0.3
# P16	Glass	$Au_{75}Pd_{25}$	3.1	3	1100	39	gl(85), pl(8), opx(3), mt(5)	3.6	3.3	-	-	0.06	0.2

[a] WR-powder:natural rock powder of IWL16; Glass:glass prepared with one-atomosphere furnace at 1,550°C

[b] H_2O content injected into sample capsule

[c] Run procedure (1) melting experiments; (2) crystallization experiments with natural rock powder as starting materials; (3) crystallization experiments with the glass as starting materials

[d] Phase proportions in weight percent are given in parentheses, calcurated by mass balance. Abbreviations of the phases: gl, glass; ol, olivine; pl, plagioclase; cpx, high-Ca pyroxene; opx, low-Ca pyroxene; mt, magnetite; Ti-mt, Ti-rich magnetite

[e] H_2O content in melt estimated by mass balance assuming H_2O is perfectly imcompatible for mineral phases. *Italic* shows H_2O-saturated runs and the H_2O content is calculated by H_2O-solubility model of Moore et al. (1998) for 1, 2 kbar and by Pele software (Boudreau 1999) for 5 kbar

[f] H_2O content in melt obtained by difference of the epma analyses of glass

[g] Experimental logfO_2 - log$fO_2$of the NNO buffer calcurated at P and T (Chou 1987). Experimental fO_2 was calculated with olivine-plagioclase oxygen barometers (Sugawara 2001) for those minerals-bearing run products and/or calculated from Fe^{3+}/Fe^{2+} ratio in melt estimated from olivine-melt equilibrium (see text). *Δ NNO estimated from olvine-melt equilibria

[h] Sum of residuals for the mass balance calculations

[i] Δ FeO is apparent loss or gain of FeO calculated as (wt%) 100*(FeO_{calc} - $FeO_{starting\ material}$)/$FeO_{starting\ material}$. For crystal-bearing run products, FeO_{calc} is concentration of FeO (total Fe as FeO) in the run product calculated by mass balance

employed for mineral phases. For glass analyses, 4–8 s counting time for Na_2O and beam sizes of 20–30 μm (rarely 5 μm for run products with small abundance of glass) were employed to avoid Na loss during the analyses. Incremental analyses on hydrous glass were also conducted to check Na loss during analyses (cf. Nielsen and Sigurdsson 1981), and the result indicates that only small Na loss (< 5% in relative) occurs under the analytical condition described above. Mass balance calculations were performed on all major oxide to estimate the proportions of phases in a given charge and evaluate the extent of Fe loss or gain. Melt H_2O contents were not analyzed directly in the present study. For H_2O-saturated charges, melt H_2O contents were calculated by H_2O solubility model of Moore et al. (1998). H_2O contents of melts in H_2O-undersaturated charge were checked for the by difference method (Devine et al. 1995).

Buffer check and determinations of fO_2

After each run at 1–2 kbar, the presence of both NiO and Ni was examined (buffer check). Buffer check of some runs at 2 kbar was conducted by powder method using the X-ray diffractometer, RINT2000 (Rigaku), installed at Department of Chemistry, Kobe University. The results show that buffer was maintained except for the runs which were carried out on low temperature (~1,000°C) and long run duration (~45 h). These failed runs are not used in this study. Buffer check of the other runs was conducted under a microscope, indicating that the oxygen fugacity might be successfully controlled near the NNO buffer in the double capsule experiments. However, because Chou and Cygan (1990) indicated that presence of a redox buffer assemblage did not necessarily mean that equilibrium redox condition was achieved, the actual oxygen fugacities in sample capsules during runs were calculated with an oxygen barometer of Sugawara (2001), which reported computer software to calculate oxygen fugacity from known chemical compositions of coexisting olivine–plagioclase at given temperature and pressure. Oxygen fugacities of some run products, which are saturated with olivine and plagioclase, were examined by this software (Table 2). The results range between NNO + 0.8 and NNO + 1.8 log unit, and the average is NNO + 1.3 log unit. Although the estimated fO_2 is much lower than that of NNO + 4 log unit estimated by Sato et al. (1999), whose experiments were carried out with the same apparatus without controlling the oxygen fugacity, the estimated NNO + 1 ± 1 log unit is slightly oxiding condition compared with NNO buffer. This failure of maintaining fO_2 at NNO buffer may be due to the high rate of hydrogen leakage through the Pt outer capsule (Chou and Cygan 1990) and usage of pure Ar as a pressure medium. Sisson and Grove (1993a, 1993b) who succeed in maintaining fO_2 at NNO used outer capsule of Au and a pressure medium of mixed Ar and methane and their non-welded sample capsule ensured the attainment of redox equilibrium.

In the experiments at 5 kbar, oxygen fugacity was not controlled to a particular buffer (e.g. iron-wustite, nickel–nickel oxide etc.), and was not calculated from the phases of run products due to absence of olivine at 5 kbar. However, both sample capsule materials and furnace assemblies used in our experiments are similar to those used in Kawamoto and Hirose (1994), who determined that the fO_2 in their experiment is NNO + 1.3 log unit. Only their Alsimag inner sleeves are different from our fired pyrophyllite inner sleeves. Therefore, we believe the oxygen fugacity is about NNO + 1 ± 1 log unit and is similar to that of the experiments at 1–2 kbar. The oxygen fugacity of NNO + 1 ± 1 log unit, the redox conditions of experiments in this study, are thus similar to the estimated values for arc basaltic-andesitic magmas (Δ NNO = 0~2, Hasenaka and Carmichael 1987; Sugawara 2001).

Results

Run products and attainment of equilibrium

Experiments were performed in the temperature and pressure ranges of 1,000–1,300°C and 1–5 kbar, respectively. Experimental conditions and results of representative runs are detailed in Table 2. Run products consisted of fluid, glass, and mineral phases. Plagioclase, low-Ca pyroxene, high-Ca pyroxene, and magnetite were observed systematically in experiments at 1–5 kbar. Olivine was only observed in experiments at 1–2 kbar and Ti-rich magnetite was only recognized in experiments at 5 kbar, respectively. The crystallinity of the run products increases as bulk H_2O content decreases at a certain temperature. Back-scattered electron images of representative run products are shown in Fig. 2, and experimental phase assemblages are listed in Table 2.

Experimental plagioclase obtained in procedure (2) and (3) is euhedral and the length is ~10–80 μm. Size of plagioclase becomes smaller (~10 μm) as the temperature decreases. High-Ca and Low-Ca pyroxenes are mostly euhedral and their size is mostly 10–50 μm. High-Ca pyroxene sometimes exhibits sector zoning in terms of alumina. Olivine is mostly euhedral. However, olivine rarely shows round shape in experiments at 2 kbar, H_2O-rich conditions (#99 and#98). Magnetite is euhedral and the average size is ~10 μm. In some run products, magnetite is very small size (< 5 μm), making the analyses difficult (Table 3).

In the early stage of this study (experiments at 2 kbar), the attainment of equilibrium was examined by utilizing both melting experiments (procedure 1) and crystallization experiments (procedure 2–3) at two run conditions (#103 versus#105,#106 versus#110; detail of the conditions of all the runs are available upon request). Runs#106 and#110 have the same phase assemblage (gl + pl + opx), and their plagioclase, which is slow

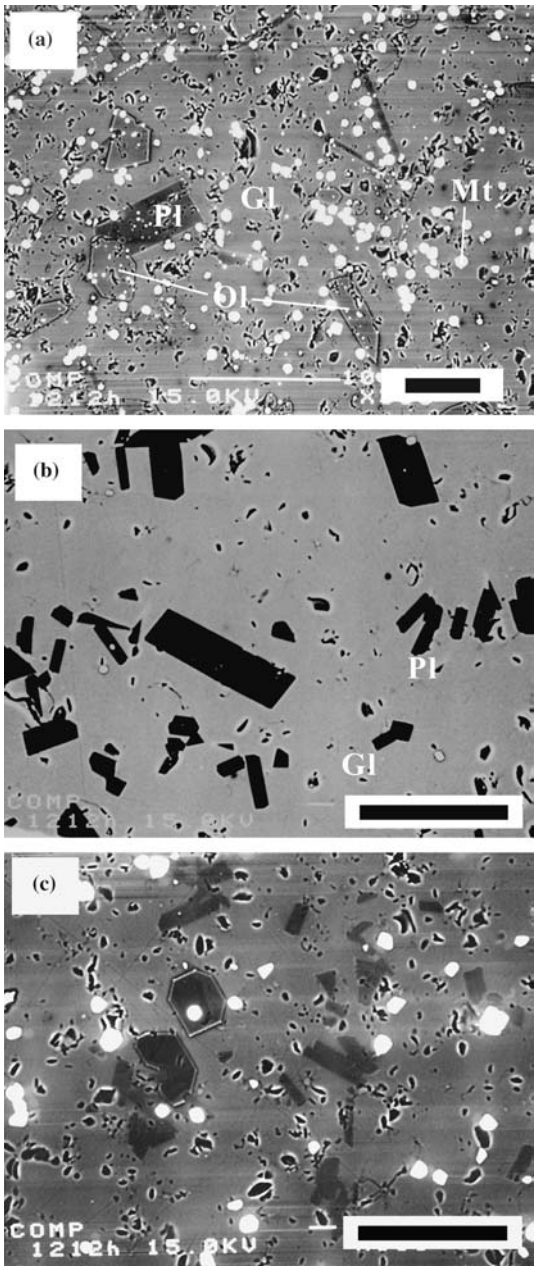

Fig. 2 Back-scattered electron images of representative run products obtained in crystallization experiments with glass as starting material (run procedure 3). **a** 1,100°C and H_2O-saturated conditions at 1 kbar (#149). **b** 1,250°C and dry conditions at 5 kbar (#P4). **c** 1,100°C and H_2O = 3.1 wt% at 5 kbar (#P16). The *horizontal black scale* is 50 μm in length. Abbreviations are *Gl*, glass; *Pl*, plagioclase; *Ol*, olivine; *Opx*, low-Ca pyroxene; *Mt*, magnetite

mineral to equilibrate, also have nearly the same composition (An_{87}), indicating that these runs attained equilibrium. Therefore, run duration about 27 h is enough for attainment of equilibrium at 1,100°C with H_2O content of 1.0 wt%. However, plagioclase compositions of run#103 and#105 at 1,150°C, which have the same phase assemblage (gl + pl), are not the same (An_{77} for#103 and An_{90} for#105). This may be due to difficulty in distinguishing between relict crystal and newly crystallized phase. The highly calcic composition of plagioclase in#105 may be derived from relict plagioclases of natural-rock powder, indicating that it is very difficult to check attainment of equilibrium by this method. In the later stage of this study (experiments at 1 kbar and 5 kbar), only procedure (3) was emplyed. It is well known that crystallization experiment are less prone to equilibration problems than melting experiment (Sisson and Grove 1993a; Martel et al. 1999; Scaillet and Evans 1999), and run durations in our experiments are systematically longer than those in Sisson and Grove (1993a, 1993b). Furthermore, all phases in run product obtained by procedure (2), (3) are homogeneous in composition (Table 3) and the mineral phases have euhedral shapes (Fig. 2), suggesting that chemical equilibrium was closely approached.

Phase relations and plagioclase compositions

The phase relations, which are constructed from the experimental data in Table 2, are represented in temperature-bulk H_2O diagrams at each pressure (Fig. 3). The phase relations at 1 kbar experiments are shown in Fig. 3a. With the increase of H_2O content, the liquidus temperature gradually decreases from 1,220°C (dry) to 1,120°C (H_2O-saturated). The liquidus phases are plagioclase at H_2O < 1 wt% and olivine and plagioclase at H_2O > 1 wt%, respectively. Olivine is stable only within 20–50°C of the liquidus at H_2O > 1 wt%, whereas plagioclase is observed in all the subliquidus run products. Saturation curves for low-Ca pyroxene and high-Ca pyroxene are 20–40°C and 60°C lower than the liquidus, respectively, and gradually decrease with increasing H_2O content to the H_2O-saturation. Magnetite crystallizes in all run products below 1,100°C.

The phase relations at 2 kbar experiments are shown in Fig. 3b. The liquidus temperature gradually decreases from 1,230°C (dry) to 1,090°C (H_2O-saturated) as bulk H_2O content increases. At H_2O < ~3 wt%, the liquidus phase is plagioclase, followed by low-Ca pyroxene and magnetite. High-Ca pyroxene crystallizes only below 1,050°C at this pressure. At H_2O > ~3 wt%, on the other hand, magnetite is the liquidus phase, followed by olivine, plagioclase, high-Ca pyroxene, and low-Ca pyroxene. Saturation curves for silicate minerals generally decrease (150–200°C) with increasing H_2O from dry to H_2O-saturated condition (~4.5 wt%).

The phase relations at 5 kbar experiments are shown in Fig. 3c. The liquidus temperature gradually decreases from 1,280°C (dry) to 1,120°C (H_2O-saturated) as bulk H_2O content increases. The saturation curve for plagioclase decreases with increasing H_2O content, and no plagioclase crystallizes at the conditions of H_2O > 7wt% and > 1,000°C. Saturation curves for low-Ca and high-Ca pyroxenes, which also decrease with increasing H_2O content, intersect that for plagioclase at H_2O ~3–4 wt%. At H_2O-saturated condition, only high-Ca

Table 3 Phase compositions of selected experiments

Sample# Phase		SiO_2		TiO_2		Al_2O_3		FeO* [b]		MnO		MgO		CaO		Na_2O		K_2O		Cr_2O_3		Total
1 kbar																						
# 133	gl[a] (5)	54.96	(24)	0.74	(3)	16.94	(9)	8.43	(35)	0.18	(2)	6.82	(14)	9.53	(7)	2.14	(8)	0.26	(1)			99.32
	pl(4)	50.55	(90)	0.09	(4)	30.42	(94)	1.32	(36)	0.01	(2)	0.74	(25)	15.47	(34)	2.36	(21)	0.04	(1)			100.98
# 129	gl(5)	54.17	(37)	0.73	(2)	16.77	(16)	9.50	(59)	0.18	(2)	6.70	(7)	9.57	(11)	2.13	(10)	0.24	(1)			97.62
	ol(5)	40.74	(28)	0.02	(2)	0.11	(10)	14.07	(53)	0.23	(3)	42.39	(52)	0.24	(4)	0.01	(1)	0.00	(0)			98.43
	pl(5)	49.36	(56)	0.02	(3)	32.67	(59)	1.26	(8)	0.02	(2)	0.27	(9)	16.81	(53)	1.80	(16)	0.02	(0)			102.22
# 148	gl(7)	56.66	(39)	0.78	(3)	16.57	(15)	8.29	(22)	0.20	(2)	5.56	(18)	9.27	(22)	2.36	(25)	0.31	(3)			97.05
	ol(7)	41.13	(21)	0.00	(1)	0.42	(53)	13.47	(34)	0.31	(4)	45.05	(68)	0.45	(33)	0.03	(2)	0.00	(0)			100.86
	pl(5)	49.31	(83)	0.06	(5)	32.20	(85)	1.53	(32)	0.01	(2)	0.40	(21)	16.81	(38)	1.85	(12)	0.03	(1)			102.21
	mt(4)	0.22	(3)	2.09	(7)	7.45	(7)	72.54	(104)	0.21	(2)	5.99	(13)	0.30	(1)	0.08	(4)	0.00	(1)	0.71	(5)	89.59
# 149	gl(7)	55.93	(33)	0.71	(2)	17.35	(21)	7.74	(26)	0.18	(3)	5.82	(14)	9.70	(6)	2.30	(16)	0.28	(1)			96.27
	ol(7)	41.50	(26)	0.01	(1)	0.03	(1)	12.42	(77)	0.26	(2)	46.92	(62)	0.21	(2)	0.02	(2)	0.00	(0)			101.37
	pl(5)	48.52	(46)	0.03	(5)	32.89	(31)	1.45	(14)	0.02	(1)	0.25	(13)	17.41	(24)	1.62	(17)	0.02	(1)			102.21
	mt(5)	0.22	(4)	1.77	(5)	8.62	(9)	72.00	(60)	0.26	(6)	7.16	(16)	0.32	(2)	0.04	(1)	0.00	(1)	1.09	(34)	91.48
2 kbar																						
# 103	gl(7)	53.61	(38)	0.72	(3)	16.70	(20)	10.00	(30)	0.18	(3)	6.57	(20)	9.61	(6)	2.34	(16)	0.26	(1)			98.24
	pl(5)	50.40	(67)	0.06	(3)	30.73	(78)	1.22	(33)	0.01	(1)	0.43	(27)	15.65	(48)	2.52	(32)	0.04	(1)			101.07
# 107	gl(7)	53.56	(15)	0.71	(4)	17.30	(15)	9.52	(12)	0.17	(4)	6.37	(13)	9.87	(3)	2.26	(13)	0.25	(1)			98.41
	pl(8)	49.08	(59)	0.06	(3)	31.53	(106)	1.36	(29)	0.02	(2)	0.52	(26)	16.65	(58)	2.10	(19)	0.03	(1)			101.35
# 66	gl(9)	54.51	(18)	0.77	(2)	17.00	(12)	8.87	(22)	0.17	(4)	6.65	(12)	9.48	(11)	2.22	(10)	0.27	(3)			95.89
	pl(8)	47.43	(32)	0.01	(2)	32.21	(27)	1.06	(10)	0.01	(2)	0.15	(3)	16.95	(33)	1.63	(11)	0.03	(1)			99.47
# 109	gl(6)	54.42	(34)	0.73	(4)	17.13	(30)	9.06	(20)	0.17	(2)	6.46	(10)	9.65	(6)	2.14	(14)	0.24	(1)			95.53
	ol(6)	40.19	(24)	0.03	(1)	0.13	(15)	13.87	(40)	0.25	(2)	43.33	(52)	0.27	(5)	0.03	(2)	0.00	(0)			99.04
	pl(6)	47.29	(38)	0.02	(2)	33.00	(40)	1.12	(5)	0.02	(2)	0.15	(4)	17.48	(29)	1.38	(12)	0.01	(1)			100.46
	mt(7)	0.18	(7)	1.36	(10)	11.21	(22)	61.65	(178)	0.60	(7)	7.35	(25)	0.29	(2)	0.10	(6)	0.00	(0)	7.00	(168)	89.74
# 116	gl(5)	55.07	(75)	0.70	(4)	17.80	(9)	8.25	(71)	0.13	(7)	5.67	(9)	10.01	(6)	2.13	(37)	0.25	(1)			93.32
	ol(10)	40.22	(40)	0.01	(1)	0.03	(2)	15.64	(90)	0.23	(3)	44.14	(56)	0.21	(3)	0.03	(4)	0.00	(1)			100.51
	pl(3)	46.82	(69)	0.01	(2)	32.97	(37)	1.27	(10)	0.01	(2)	0.16	(3)	17.41	(38)	1.29	(13)	0.02	(1)			99.95
	mt(4)	0.16	(2)	1.75	(13)	8.55	(14)	69.53	(192)	0.29	(3)	6.51	(8)	0.29	(2)	0.00	(0)	0.01	(1)	3.93	(81)	91.01
# 64	gl(9)	59.78	(112)	0.77	(5)	17.22	(71)	6.69	(73)	0.19	(3)	4.38	(45)	8.55	(50)	2.07	(34)	0.34	(4)			95.45
	ol(11)	40.36	(37)	0.01	(1)	0.05	(5)	16.93	(141)	0.36	(3)	43.54	(109)	0.22	(4)	0.01	(1)	0.01	(1)			101.48
	pl(3)	46.47	(47)	0.02	(0)	33.89	(28)	0.78	(8)	0.03	(3)	0.09	(2)	18.22	(27)	1.25	(9)	0.02	(1)			100.76
	cpx(2)	53.96	(13)	0.24	(2)	2.04	(11)	6.79	(35)	0.29	(4)	18.05	(29)	19.38	(83)	0.21	(4)	0.00	(0)			100.96
	opx(7)	54.93	(77)	0.15	(4)	2.10	(90)	10.28	(97)	0.31	(3)	30.03	(108)	1.80	(16)	0.04	(5)	0.00	(0)			99.64
	mt(8)	0.10	(2)	2.25	(19)	5.78	(11)	77.15	(175)	0.28	(3)	6.32	(13)	0.22	(4)	0.06	(10)	0.00	(1)			92.77
5 kbar																						
# P4	gl(7)	53.82	(17)	0.75	(3)	16.11	(32)	10.26	(22)	0.16	(3)	7.07	(15)	9.41	(8)	2.17	(3)	0.26	(1)			98.39
	pl(9)	51.38	(28)	0.03	(3)	28.68	(27)	1.51	(14)	0.02	(1)	0.27	(7)	14.01	(18)	3.09	(14)	0.06	(1)			99.05
# P15	gl(6)	56.27	(30)	0.81	(2)	15.67	(29)	8.65	(32)	0.21	(3)	6.36	(13)	9.54	(9)	2.20	(6)	0.29	(1)			97.21
	pl(8)	50.93	(45)	0.03	(3)	29.81	(56)	1.88	(25)	0.02	(2)	0.29	(11)	14.74	(34)	2.70	(18)	0.05	(1)			100.45
	opx(4)	52.64	(28)	0.14	(1)	5.94	(37)	9.24	(33)	0.28	(3)	30.09	(28)	1.52	(21)	0.06	(4)	0.01	(0)			99.91
	mt(6)	0.19	(2)	0.78	(3)	8.58	(37)	70.85	(65)	0.32	(4)	9.92	(34)	0.25	(1)	0.05	(6)	0.00	(1)	0.67	(6)	91.61
# P9	gl(8)	56.54	(47)	0.75	(3)	16.78	(18)	6.85	(31)	0.18	(3)	6.35	(14)	9.95	(7)	2.30	(9)	0.28	(1)			96.25
	pl(12)	49.95	(51)	0.01	(1)	30.65	(30)	1.63	(11)	0.01	(1)	0.22	(1)	15.41	(30)	2.48	(17)	0.03	(1)			100.39
	opx(4)	53.50	(94)	0.17	(4)	5.57	(79)	7.65	(45)	0.26	(3)	30.52	(96)	1.91	(36)	0.05	(4)	0.01	(1)			99.64
	mt(5)	0.13	(1)	0.76	(5)	9.70	(76)	68.74	(79)	0.34	(2)	11.62	(37)	0.25	(3)	0.02	(3)	0.00	(0)	0.47	(6)	92.02
# P16	gl(5)	56.50	(20)	0.69	(2)	16.97	(13)	7.07	(14)	0.20	(5)	6.16	(10)	9.77	(9)	2.36	(8)	0.27	(1)			96.71
	pl(7)	49.17	(32)	0.02	(2)	31.06	(33)	1.60	(11)	0.02	(2)	0.21	(2)	15.78	(16)	2.17	(11)	0.03	(1)			100.05
	opx(4)	52.92	(15)	0.13	(2)	5.99	(30)	8.23	(54)	0.25	(2)	30.70	(31)	1.53	(4)	0.03	(3)	0.00	(0)			99.77
	mt(5)	0.18	(1)	0.78	(4)	9.36	(37)	69.70	(73)	0.34	(4)	10.96	(9)	0.23	(2)	0.04	(3)	0.00	(1)	0.46	(2)	92.04

Abbreviations as in Table 2; Number in parentheses in the phase column gives the number of analyses; Numbers in parentheses in the oxide columns are the standard deviation*100

[a] Glass analyses normalized to 100% anhydrous. Unnormalized total is reported

[b] FeO* is total Fe as FeO

[c] Very small (< 5 micron) magnetite. The composition may be contaminated by sorrounding glass during analyses

pyroxene is stable silicate mineral at ~1,000°C. Ti-rich magnetite, which crystallizes only at 5 kbar, is stable at low temperature and low-H_2O conditions. No olivine crystallizes at 5 kbar experiments. The stability field of olivine exists only in H_2O-rich regions near the liquidus at 2 kbar (Fig. 3b) and enlarges toward lower-H_2O region as the experimental pressure decreases to 1 kbar (Fig. 3a). This characteristic is consistent with well-known effects of pressure and H_2O on olivine stability relative to orthopyroxene.

Phase compositions of selected runs are presented in Table 3. Complete table of phase analyses for successful runs are available upon request to the authors. The compositional range of experimental plagioclase is between An_{67} and An_{89}, which decreases with decreasing temperature and H_2O content and increasing pressure.

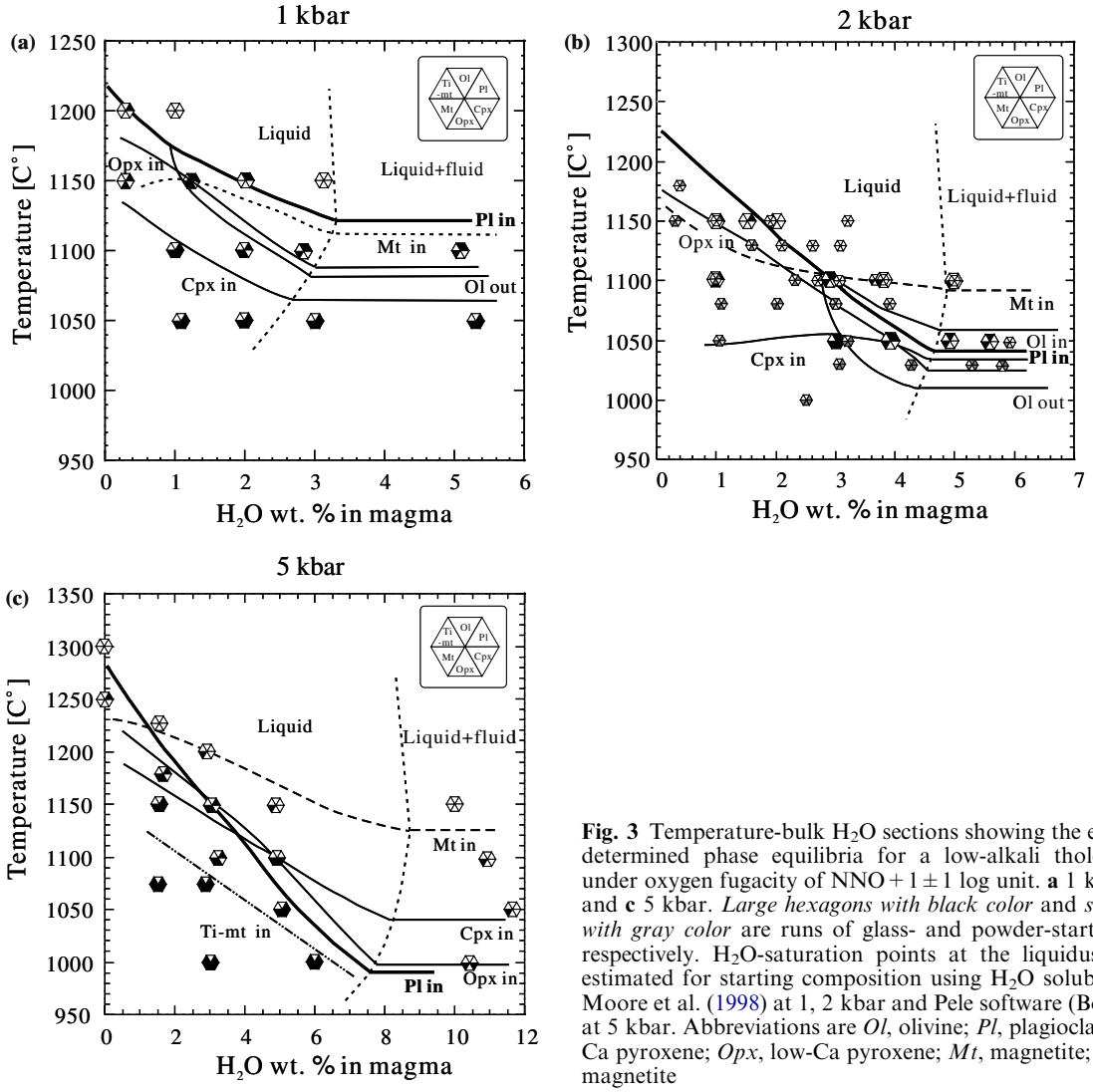

Fig. 3 Temperature-bulk H_2O sections showing the experimentally determined phase equilibria for a low-alkali tholeiite (IWL16) under oxygen fugacity of NNO + 1 ± 1 log unit. **a** 1 kbar, **b** 2 kbar, and **c** 5 kbar. *Large hexagons with black color* and *small hexagons with gray color* are runs of glass- and powder-starting materials, respectively. H_2O-saturation points at the liquidus are roughly estimated for starting composition using H_2O solubility model of Moore et al. (1998) at 1, 2 kbar and Pele software (Boudreau 1999) at 5 kbar. Abbreviations are *Ol*, olivine; *Pl*, plagioclase; *Cpx*, high-Ca pyroxene; *Opx*, low-Ca pyroxene; *Mt*, magnetite; *Ti-mt*, Ti-rich magnetite

The most calcic plagioclase is obtained at 2 kbar, 1,030°C and H_2O-saturated condition. An contents of near-liquidus plagioclases and the K_D^{Ca-Na} are presented in Table 4 with CaO/Na_2O and Al_2O_3/SiO_2 ratios of the coexisting melt, and are used in the following discussion. Figure 4 compares the H_2O contents in liquid by two methods; one is obtained by mass balance calculation assuming H_2O is perfectly incompatible for mineral phases and H_2O is retained in the capsule, the other is by difference method of epma analyses of glass. The figure substantiate the appropriateness of the calculated H_2O content within the error of the by difference method.

Discussion

Effect of H_2O content on Ca–Na partitioning between plagioclase and melt

Previous experimental studies of plagioclase-melt equilibria demonstrated that melt Al_2O_3/SiO_2 and CaO/Na_2O ratios, H_2O contents, temperature, and pressure affect the An content of plagioclase (Housh and Luhr 1991; Sisson and Grove 1993a; Longhi et al. 1993; Panjasawatwong et al. 1995). Because experiments in this study were performed on only one composition, compositional range of melts coexisting with the liquidus plagioclases is expected to be small. Actually, compositional ranges of CaO/Na_2O and Al_2O_3/SiO_2 ratios in the melts are 3.97–4.70 ($4.32 \pm 0.15\sigma$) and 0.279–0.323 ($0.305 \pm 0.011\sigma$), respectively, indicating restricted compositional ranges (Fig. 1, Fig. 5a, b; Table 4). Furthermore, the An-CaO/Na_2O and An-Al_2O_3/SiO_2 diagrams show no correlation between them (Fig. 5a, b), suggesting that there is not sufficient variation in the melt CaO/Na_2O and Al_2O_3/SiO_2 ratios in the present experiments to affect An in plagioclase. Experimental temperature shows a correlation with An content (Fig. 5c), however, liquidus temperature also decreases with increasing H_2O content (e.g. Danyushevsky 2001). Therefore, variation of An content of plagioclase obtained near the liquidus conditions at

Table 4 An content of plagioclase crystallized near the liquidus conditions, the composition of the coexisting melt, and K_D^{Ca-Na} between plagioclase and the coexisting melt

	Conditions			Plagioclase	Melt		
Sample#	T (°C)	Melt H_2O (wt%)	Phases	An (mol%)	CaO/Na_2O	Al_2O_3/SiO_2	K_D^{Ca-Na}
1 kbar							
# 133	1200	0.3	gl(98), pl(2)	78.4	4.46	0.308	1.5
# 129	1150	2.1	gl(95), ol(1), pl(4)	83.8	4.51	0.310	2.1
# 148	1100	3.3	gl(80), ol(4), pl(13), mt(3)	83.4	3.97	0.292	2.3
# 149	1100	3.3	gl(88), ol(3), pl(6), mt(3)	85.6	4.23	0.310	2.6
2 kbar							
# 103	1150	1.0	gl(96), pl(4)	77.4	4.13	0.312	1.5
# 107	1150	1.5	gl(100), pl(tr)	81.4	4.38	0.323	1.8
# 66	1130/1100	2.8	gl(98), pl(2)	85.2	4.28	0.312	2.4
# 109	1100	3.1	gl(94), ol(1), pl(3), mt(2)	87.5	4.50	0.315	2.8
# 116	1050	4.2	gl(93), ol(3), pl(2), mt(2)	88.2	4.70	0.323	2.9
# 64	1050/1030	4.9	gl(67), ol(4), pl(16), cpx(6), opx(2), mt(5)	89.0	4.12	0.288	3.5
5 kbar							
# P4	1250	0.0	gl(91), pl(9)	71.5	4.34	0.299	1.0
# P15	1180	2.1	gl(75), pl(17), opx(5), mt(3)	75.1	4.34	0.279	1.3
# P9	1150	3.5	gl(85), pl(8), opx(2), mt(5)	77.5	4.33	0.297	1.4
# P16	1100	3.6	gl(85), pl(8), opx(3), mt(5)	80.1	4.14	0.300	1.8

given pressure depends on the H_2O content in the coexisting melt.

Variations of An content of near-liquidus plagioclase and of the K_D^{Ca-Na} with melt H_2O content are shown in Fig. 6. An content of plagioclase obtained at dry condition ($H_2O = 0$) decreases with increasing experimental pressure (Fig. 6a), which is consistent with previously demonstrated pressure dependence of plagioclase-melt equilibria at dry condition (e.g. Longhi et al. 1993; Panjasawatwong et al. 1995), and increase of melt H_2O content can make near-liquidus plagioclases more anorthitic up to 7, 12, and 9 mol% at 1, 2, and 5 kbar, respectively (Fig. 6a). It is difficult to discriminate between the individual effects of melt H_2O and temperature on An content and K_D^{Ca-Na}, however, it appears that both An content of the near-liquidus plagioclase and the K_D^{Ca-Na} almost linearly increase as melt H_2O content increases at each pressure (Fig. 6). These results suggest that, when CaO/Na_2O and Al_2O_3/SiO_2 ratios of the coexisting melt are nearly constant, An content of liquidus plagioclase and the K_D^{Ca-Na} can be expressed by linear equations containing only melt H_2O content as a variable at given pressure. In order to account for the effects of temperature and pressure, least square regressions (LLSQ of Sugawara 1999) with An content and K_D^{Ca-Na} variations from our 1–5 kbar experiments as dependent variables were carried out with the following results:

$$\ln \mathrm{An} = 927.91/T(\mathrm{K}) - 0.86298 - 0.02693 \times P(\mathrm{bar})/T(\mathrm{K}) + 0.01674 \times \mathrm{H_2O\ (wt.\%)}$$
$$r = 0.966, \quad (1)$$

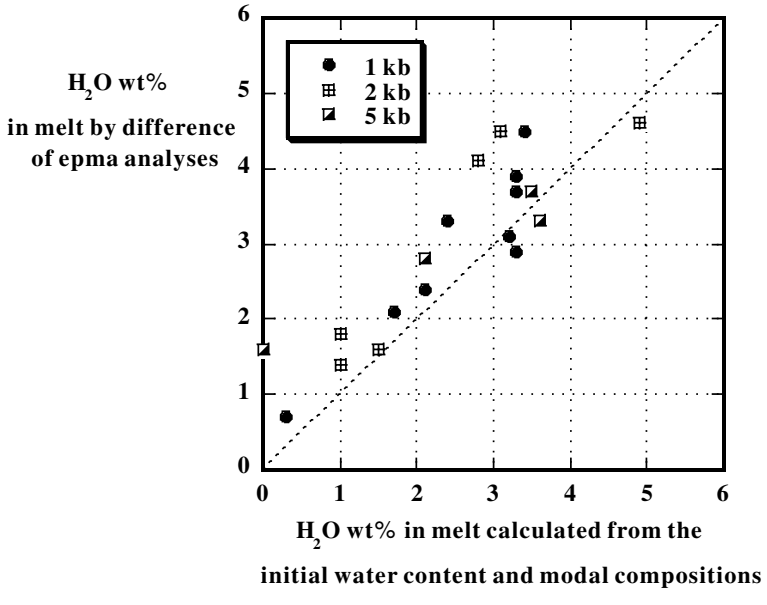

Fig. 4 H_2O contents in liquid by two methods; one is estimated by mass balance calculation assuming H_2O is perfectly incompatible for mineral phases, the other is by difference method of epma analyses of glass

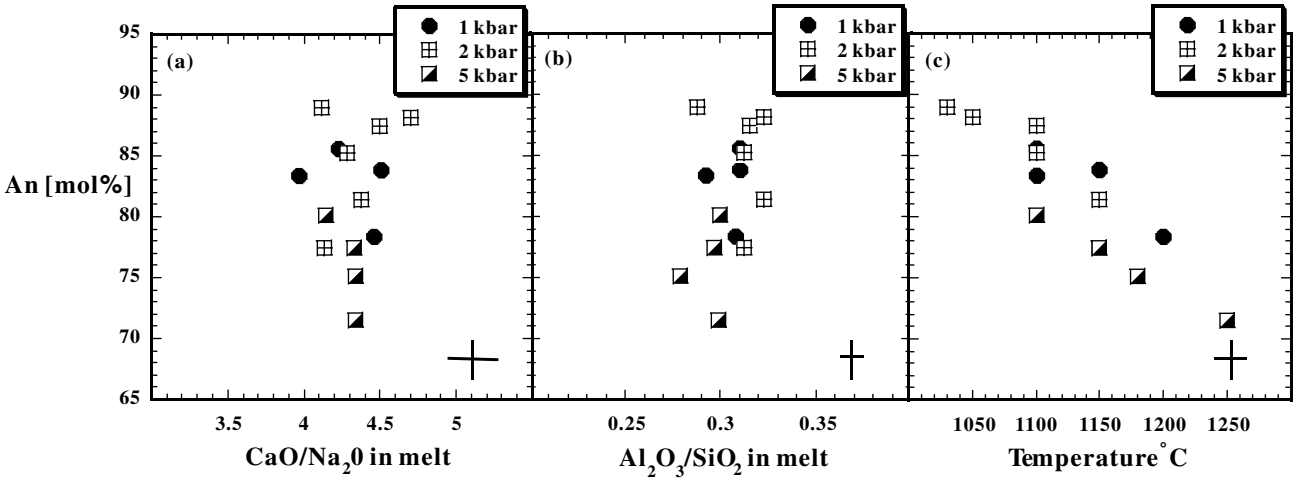

Fig. 5 Variations of An content of plagioclase obtained near the liquidus condition with **a** melt CaO/Na_2O, **b** melt Al_2O_3/SiO_2, and **c** experimental temperature. Observed variation of An contents of near-liquidus plagioclases does not depend on melt CaO/Na_2O, Al_2O_3/SiO_2 ratios, but on temperature. *Error bars* show one standard deviation

$$\ln K_D^{\text{Ca-Na}} = 10695/T(\text{K}) - 6.7781 - 0.1009 \times P(\text{bar})/T(\text{K}) - 0.00860 \times \text{H}_2\text{O}(\text{wt.\%})$$
$$r = 0.969, \qquad (2)$$

where r is the correlation coefficient. The standard deviations (1σ) of An and $K_D^{\text{Ca-Na}}$ determined from these equations are 1.4 mol% and 0.19, respectively. We emphasize that these equations cannot be applied to describe plagioclase-melt equilibria outside the compositional range of our experiments for which it is indispensable to include effect of melt composition. However, these formulations will become the basis for subsequent formulations that include effects of melt composition and can be applicable to a wide compositional range.

Because our experimental results indicate that the effect of H_2O on $K_D^{\text{Ca-Na}}$ is dependent on the experimental pressure (Fig. 6b), for comparing our results with those of previous studies, we must make the comparison of $K_D^{\text{Ca-Na}}$ obtained at the same experimental pressure. Our 1–5 kb data for $K_D^{\text{Ca-Na}}$ versus melt H_2O content at 1, 2, and 5 kbar are presented in Fig. 7 together with data of Sisson and Grove (1993a, 1993b), Baker and Eggler(1987) and Panjasawatwong et al. (1995). Although the compiled $K_D^{\text{Ca-Na}}$ for HABs compositions are scattered even at given melt H_2O content, the $K_D^{\text{Ca-Na}}$ for HABs show systematically higher values than those obtained on low-alkali tholeiite in this study at the same experimental pressure, indicating that there are some compositional effects (e.g. Al_2O_3/SiO_2) on $K_D^{\text{Ca-Na}}$.

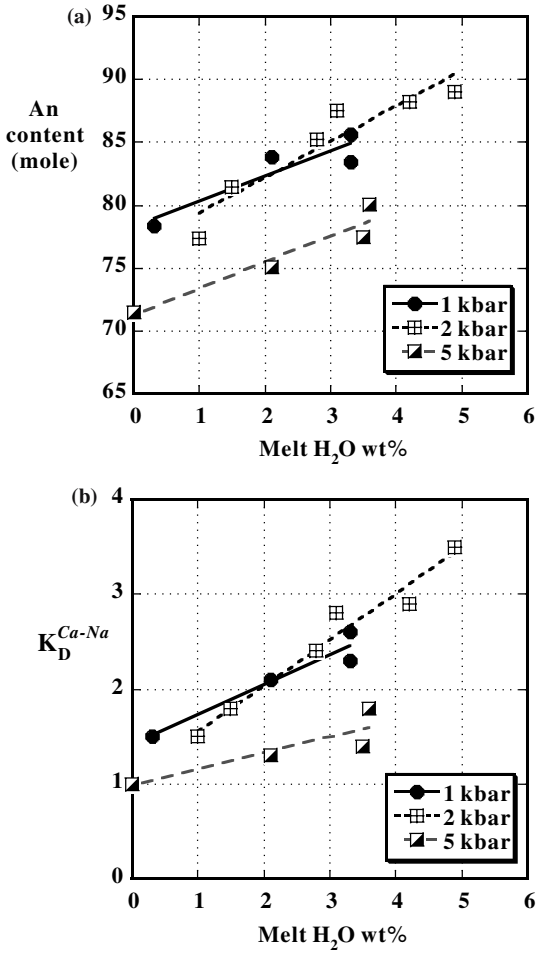

Fig. 6 Effect of H_2O on **a** An content of near-liquidus plagioclase and **a**$K_D^{\text{Ca-Na}}$ between the plagioclase and the coexisting melt at 1 kbar, 2 kbar, and 5 kbar. *Lines* represent regression line at each pressure. In **a** at 1 kbar; An = 78.3 + 2.0×(H_2O), r = 0.914: at 2 kbar; An = 75.9 + 2.9×(H_2O), r = 0.960: at 5 kbar; An = 71.2 + 2.1×(H_2O), r = 0.959. In **b** at 1 kbar; $K_D^{\text{Ca-Na}}$ = 1.41 + 0.32×(H_2O), r = 0.964: at 2 kbar; $K_D^{\text{Ca-Na}}$ = 1.04 + 0.50×(H_2O), r = 0.967: at 5 kbar; $K_D^{\text{Ca-Na}}$ = 1.05 + 0.13×(H_2O), r = 0.946

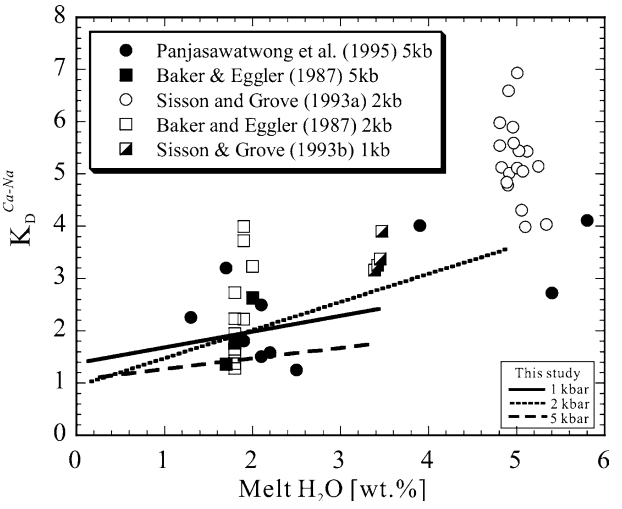

Fig. 7 Variations of K_D^{Ca-Na} with melt H_2O content in basaltic composition at 1 kbar, 2 kbar, and 5 kbar from literatures. *Lines* represent regression lines for low-alkali tholeiite at each pressure obtained in this study (Fig. 6b). Melt H_2O content of H_2O-saturated experiments of Sisson and Grove (1993a, 1993b) are determined by H_2O solubility model of Moore et al. (1998)

What conditions does most An-rich plagioclase crystallize?

The An contents and K_D^{Ca-Na} variations for near-liquidus plagioclase with pressure and melt H_2O content are shown on Fig. 8. The variations observed in Fig. 8 are derived mostly from the effects of melt H_2O content, temperature, and pressure as described in Eqs. (1) and (2). Isopleths for An content and K_D^{Ca-Na} fitted by hand are also drawn on Fig. 8. Both the An content and the K_D^{Ca-Na} increase with increase of melt H_2O content and decrease with the pressure, indicating that the most An-rich plagioclase ($\sim An_{90}$, maximum $An_{92.5}$) crystallizes from the low-alkali tholeiitic melt, near the H_2O-saturated pressure of 2–3 kbar. These pressure ranges are also important in terms of the crystallization of olivine or Ca-rich clinopyroxene. At 2 kbar, olivine is the liquidus phase in H_2O-rich compositions, crystallization of which does not affect the CaO/Na_2O ratio of the melt, and An-rich plagioclase may crystallize in the subliquidus conditions, whereas crystallization of Ca-rich clinopyroxene at 5 kbar water-rich conditions may decrease the CaO/Na_2O ratio of the subliquidus melt, from which less An-rich plagioclase may crystallize. Therefore, pressure ranges of 2–3 kbars are optimal in terms of element partitioning and phase equilibrium relations for the crystallization of An-rich plagioclase.

Panjasawatwong et al. (1995) suggested, based on their H_2O-undersaturated experiments at 5 kbar and H_2O-saturated experiments at 2 kbar of Sisson and Grove (1993a), that the actual achievement of H_2O-saturated conditions exerts a much stronger influence

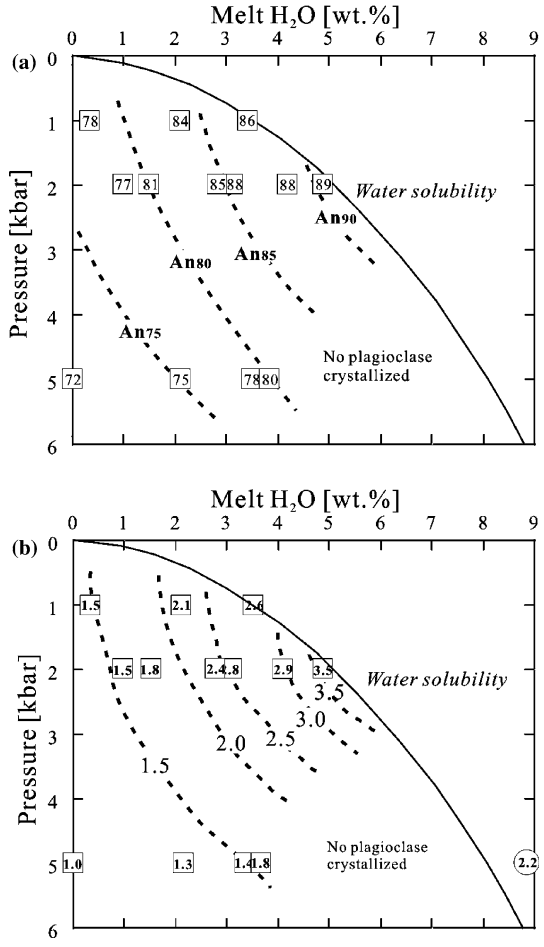

Fig. 8 Variations of **a** An content and **b** K_D^{Ca-Na} for near-liquidus plagioclase with pressure and melt H_2O content. *Number in square* represents obtained An content and K_D^{Ca-Na} at the condition. *Solid line* represents H_2O saturation curve for starting composition estimated by the model of Moore et al. (1998). *Dashed lines* are fitted by hand

on plagioclase composition than increasing amount of H_2O in H_2O-undersatureted conditions: plagioclase crystallized from H_2O-saturated melt becomes more anorthitic than that from significantly H_2O-undersaturated melt even at the same H_2O content. This idea is thermodynamically irrelevant because saturation/undersaturation do not matter with the equilibrium partitioning between melt and plagioclase as illustrated by nearly linear An and K_D^{Ca-Na} (Figs. 5, 7a). Danyushevsky et al. (1997) conducted detailed petrological and melt inclusion studies of high-Ca boninite, and suggested that phenocrysts of An-rich plagioclase ($An_{>90}$) crystallized at the last stages of melt evolution from H_2O-saturated dacitic melts (SiO_2 ~64–67 wt%, MgO ~2 wt%, H_2O ~1.5 wt%, and CaO/Na_2O ~3) at the pressure of < 1 kbar. However, such an An-rich plagioclase would not crystallize at pressure of < 1 kbar at least in the tholeiitic composition used in the present study (SiO_2 ~53 wt%, CaO/Na_2O ~4.2, and Al_2O_3/SiO_2 ~0.3).

Applications for the crystallization condition of An-rich plagioclase in arc magmas

An-rich plagioclases ($>An_{90}$) are commonly observed in arc basalts (Bloomer et al. 1989; Avdeiko et al. 1991; Singer et al. 1993; Kimata et al. 1995; Tsukui and Hoshino 2002; A-Miyasaka and Nakagawa 2002). Although the An-rich plagioclases are regarded as xenocrysts in some cases (Kimata et al. 1995; A-Miyasaka and Nakagawa 2002), even the plagioclase xenocrysts should have crystallized from melts with arc-related melt compositions at certain physical conditions. The crystallization pressures and melt H_2O contents as well as melt compositions have remained obscure.

MORB-like low H_2O concentrations (0.21–0.38 wt%) in primary magmas, which are evidence for pressure-release melting, are reported in a few cases (Sisson and Bronto 1998). For the origin of An-rich plagioclase ($<An_{95}$) in such a low H_2O concentration basalts (Gerbe et al. 1992), the high CaO/Na_2O (~5–7) and high Al_2O_3 (18–21 wt%) in melts (Sisson and Bronto 1998) may be responsible as suggested by Panjasawatwong et al. (1995). However, for many cases, it is widely considered that hydrous fluid phase released from subducted oceanic crust and sediment to mantle wedge plays an important role for the origin of high-MgO low-alkali tholeiitic basalts in arc volcanic fronts (Tatsumi 1989; Ishikawa and Nakamura 1994; Shibata and Nakamura 1997). Recent studies for glass inclusions in magnesian olivine phenocrysts show that primary melts of arc tholeiitic magmas (~8–12 wt% MgO) contain at least 2.0–2.5 wt% H_2O (Sobolev and Chaussidon 1996). Starting from the most primitive melt compositions (~12 wt% MgO), 30–50% fractional crystallization of anhydrous minerals lead to form evolved tholeiitic melts with 3.5–5.0 wt% H_2O. In fact, some glass inclusions with evolved arc tholeiitic compositions (~5–7 wt% MgO) in olivine phenocrysts, which coexist with An-rich plagioclases (up to An_{93}), contain H_2O contents of 3–6 wt% at crustal pressure (Roggensack et al. 1997). This is consistent with low MgO content of An-rich plagioclases in arc basalts (~0.03–0.15wt%: Kuritani 1998; Takagi unpublished data). The MgO contents of those plagioclases are systematically lower than those of plagioclase in MORBs (ca. 0.2–0.4 wt%: Kuo and Kirkpatrick 1982; Sato 1989), suggesting that An-rich plagioclase in arc basalt are derived from slightly evolved melts by crystallization of magnesian olivine. From the discussion above, near H_2O-saturated condition at 2–3 kbar, which is an optimal condition for the crystallization of most An-rich plagioclase ($>An_{90}$) suggested by our experiments, are thought to be achieved in some part of crustal magma chamber at 7–11 km depth. Therefore, we believe that An-rich plagioclases observed in low-alkali tholeiite crystallized from tholeiitic melts (CaO/Na_2O~3–7, Al_2O_3/SiO_2 ~0.25–0.38) at H_2O-rich part of crustal magma chamber.

For HABs, which are another dominant volcanic products in volcanic front, Sisson and Grove (1993b) demonstrated experimentally that HABs could have contained H_2O content of 4–6 wt%. This high H_2O content in HABs is confirmed by direct measurement of glass inclusions in olivine phenocrysts from Mt. Fuego HABs (Sisson and Layne 1993). An-rich plagioclase ($>An_{90}$) can crystallize from such melts under H_2O-saturated conditions at 2 kbar with ~5 wt% H_2O (Sisson and Grove 1993a). For HABs composition, as the case for low-alkali tholeiite, it seems that H_2O-saturated condition at 2–3 kbar is preferable for crystallization of most An-rich plagioclase (Fig. 8). Although further experimental verification is required, we suggest that An-rich plagioclases in HABs crystallized from H_2O-rich melt in crustal magma chamber at 2–3 kbar.

Panjasawatwong et al. (1995) suggested the existence of extremely high CaO/Na_2O (>8) melts to account for the presence of An-rich plagioclases ($>An_{90}$) in arc-related tholeiitic basalts. Their hydrous experiments were conducted at 5 and 10 kbar, and may be affected by the lowering of An content of liquidus plagioclase due to the effect of pressure and crystallization of Ca-rich clinopyroxene. The present study demonstrated that the maximum An content of liquidus plagioclase appears at 2–3 kbar near water-saturated conditions for an arc tholeiite, and crystallization of such An-rich plagioclase (An_{90-94}) does not require anomalously refractory melts. Figure 9 shows the isopleths of An content of plagioclase in terms of partition coefficient, K_D^{Ca-Na} and CaO/Na_2O ratio of melt. The figure illustrates that An-rich plagioclase (An_{90-94}) can crystallize from normal arc tholeiite (CaO/Na_2O = 3–7; Fig. 1) at K_D^{Ca-Na} = 3–4, which are achieved at H_2O-saturated condition of 2–3 kbar. Therefore, we presume that the An-rich plagioclase (An_{90-94}) crystallized from hydrous melts rather than anomalously high CaO/Na_2O melt. However, some of arc tholeiites contain extremely An-rich plagioclases (An_{96-98}; Arakawa et al. 1992; Kimata et al. 1995). Available Ca-Na partition coefficients, as discussed

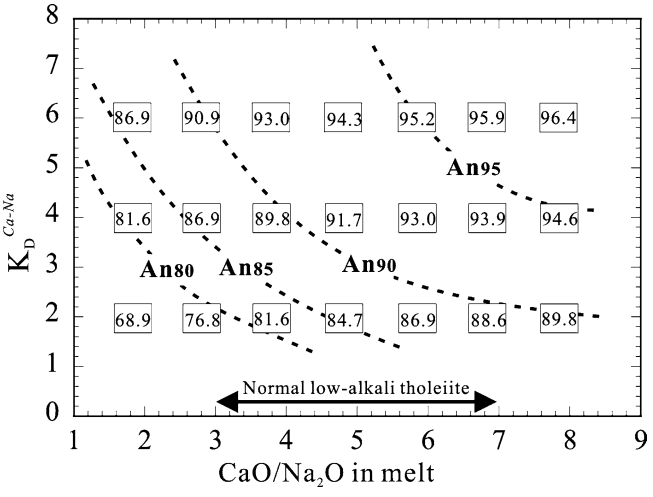

Fig. 9 Isopleths of An content of plagioclase in terms of partition coefficient K_D^{Ca-Na} and melt CaO/Na_2O ratio. *Dashed lines* are fitted by hand. See text for discussion

previously, suggest that such extremely An-rich plagioclases are out of partition equilibrium with normal arc tholeiites ($CaO/Na_2O = 3–7$; Fig. 1) (Fig. 9). Thus, anomalously high CaO/Na_2O (>8) melts might be responsible for the origin of such an extremely An-rich plagioclase as suggested by Panjasawatwong et al. (1995).

Conclusions

We documented the effects of melt H_2O content, temperature, and pressure on the Ca–Na partitioning between plagioclase and low-alkali tholeiitic melt at oxygen fugacities appropriate to subduction zone magmas by keeping melt Ca/Na_2O and Al_2O_3/SiO_2 ratios constant. Main conclusions in the present study are as follows:

1. An content and K_D^{Ca-Na} variations on liquidus surface of pressure-melt H_2O section are constructed for a low-alkali tholeiite (IWL16). Both of them increase with increasing melt H_2O and decreasing pressure, indicating that nearly H_2O-saturated conditions of 2–3 kbar is optimal for the crystallization of the most An-rich plagioclase ($\sim An_{90}$, maximum $An_{92.5}$; $K_D^{Ca-Na} = 3.8$) in arc tholeiite.
2. The variations of An content and K_D^{Ca-Na} described in (2) are expressed successfully by Eqs. 1 and 2 that include temperature, pressure, and melt H_2O content as variables.
3. K_D^{Ca-Na} variations obtained in our experiments combined with estimated H_2O content for arc tholeiitic magmas suggest that An-rich plagioclases ($An_{90–94}$) in low-alkali tholeiite crystallized from normal tholeiitic melts ($CaO/Na_2O \sim 3–7$) in H_2O-rich part of crustal magma chamber at a depth of 7–11 km.

Acknowledgements This paper formed a part of D. Takagi's Master thesis at Kobe University, Japan. We thank Dr. Toru Sugawara for valuable discussion and constructive review on an early version of the manuscript. Journal reviews of Prof. John Longhi and an anonymous reviewer, and editorial suggestions by Prof. Tim Grove were of much help to improve the contents of the paper. We are indebted to Profs. K. Uto, K. Suzuki-Kamata and all the members of Volcanology Group at Kobe University for constructive discussions and encouragement throughout this study. The technical assistance of Mr. K. Sangen during high-pressure experiments with piston cylinder and of N. Tomioka during the EPMA analyses are acknowledged. This work was financially supported in part by Grant-in-Aid for Scientific Research from the Japan Society for the Promotion of Science to H. Sato.

References

Akella J, Vaidya SN, Kennedy GC (1969) Melting of sodium chloride at pressures to 65 kbar. Phys Rev 185:1135–1140

A-Miyasaka M, Nakagawa M (2002) Origin of Anorthite and olivine phenocrysts in island-arc tholeiite: petrological study of 1940 and 1962 ejecta from Miyake-jima volcano, Izu-Mariana arc. J Volc Geotherm Res 117:263–283

Arakawa Y, Murakami H, Kimata M, Shimoda S (1992) Strontium isotope compositions of Anorthite and olivine phenocrysts in basaltic lavas and scorias of Miyakejima volcano, Japan. J Min Petr Econ Geol 87:226–39

Arculus RJ, Wills KJA (1980) The petrology of plutonic blocks and inclusions from the Lesser Antilles island arc. J Petrol 21:743–799

Avdeiko GP, Volynets ON, Antonov AYu, Tsvetkov AA (1991) Kurile island-arc volcanism: structural and petrological aspects. Techtonophys 199:271–287

Baker DR, Eggler DH (1987) Compositions of anhydrous and hydrous melts coexisting with plagioclase, augite, and olivine or low-Ca pyroxene from 1 atm to 8 kbar: application to the Aleutian volcanic center of Atka. Am Mineral 72:12–28

Beard JS, Borgia A (1989) Temporal variation of mineralogy and petrology in cognate gabbroic enclaves at Arenal volcano, Costa Rica. Contrib Mineral Petrol 103:110–122

Bloomer SH, Stern RJ, Fisk E, Geschwind CH (1989) Shoshoniitc volcanizm in the northern Mariana arc 1. Mineralogic and major and trace element characteristics. J Geophys Res 94:4469–4496

Chou I-M (1987) Oxygen buffer and hydrogen sensor techniques at elevated pressures and temperature. In: Barnes HL, Ulmer GC (ed) Hydrothermal experimental techniques. John Wiley, New York, pp 61–99

Chou I-M, Cygan GL (1990) Quantitative redox control and measurement in hydrothermal experiments. In: Spencer RJ and Chou I-M (ed) Fluid-mineral interaction: a tribute to H. P. Eugster. The Geochemi Soc, Special Pub No. 2:3–15

Danyushevsky LV (2001) The effect of small amounts of H_2O on crystallization of mid-ocean ridge and backarc basin magmas. J Volc Geotherm Res 110:265–280

Danyushevsky LV, Carroll MR, Falloon TJ (1997) Origin of high-An plagioclase in Tongan high-Ca boninites: implications for plagioclase-melt equilibria at low P(H_2O). Can Mineral 35:313–326

Devine JD, Gardner JE, Brack HP, Layne GD, Rutherford MJ (1995) Comparison of microanalytical methods for estimating H_2O contents of silicic volcanic glasses. Amer Mineral 80:319–328

Duncan RA, Green DH (1987) The genesis of refractory melts in the formation of oceanic crust. Contrib Mineral Petrol 96:326–342

Gerbe MC, Gourgaud A, Sigmarsson O, Harmon RS, Joron JL, Provost A (1992) Mineralogical and geochemical evolution of the 1982–1983 Galunggung eruption (Indonesia). Bull Volc 54:284–298

Gill J, Whelan P (1989) Early rifting of an oceanic island arc (Fiji) produced shoshonitic to tholeiitic basalts. J Geophys Res 94:4561–4578

Hasenaka T, Carmichael ISE (1987) The cinder cones of Michoacan-Guanajuato, central Mexico: petrology and chemistry. J Petrol 28:241–269

Housh TB, Luhr JF (1991) Plagioclase-melt equilibria in hydrous systems. Am Mineral 76:477–492

Ishikawa T, Nakamura E (1994) Origin of the slab component in arc lavas from across-arc variation of B and Pb isotopes. Nature 370:205–208

Kawamoto T, Hirose K (1994) Au-Pd sample containers for melting experiments on iron and water bearing systems. Eur J Mineral 6:381–385

Kimata M, Nishida N, Shimizu M, Saito S, Matsui T, Arakawa Y (1995) Anorthite megacrysts from island arc basalt. Mineral Mag 59:1–14

Kuo L-C, Kirkpatrick RJ (1982) Pre-eruption history of phyric basalts from DSDP Legs 45 and 46: evidence from morphology and zoning patterns in plagioclase. Contrib Mineral Petrol 79:13–27

Kuritani T (1998) Boundary layer crystallization in a basaltic magma chamber: evidence from Rishiri Volcano, northern Japan. J Petrol 39:1619–1640

Longhi J, Fram MS, Auwera JV, Montieth JN (1993) Pressure effects, kinetics, and rheology of anorthositic and related magmas. American Mineralogist 78:1016–1030

Martel C, Pichavant M, Holtz F, Scaillet B, Bourdier J-L, Traineau H (1999) Effects of fO_2 and H_2O on andesite phase relations between 2 and 4 kbar. J Geophys Res 104:29453–29470

Metrich N, Rutherford MJ (1998) Low pressure crystallization paths of H_2O-saturated basaltic-hawaiitic melts from Mt Etna: implications for open-system degassing of basaltic volcanoes. Geochim Cosmochim Acta 62:1195–1205

Mirwald PW, Kennedy GC (1979) The melting curve of gold, silver, and copper to 60-kbar pressure: a reinvestigation. J Geophys Res 84:6750–6756

Moore G, Carmichael ISE (1998) The hydrous phase equilibria (to 3 kbar) of an andesite and basaltic andesite from western Mexico: constrains on water content and conditions of phenocryst growth. Contrib Mineral Petrol 130:304–319

Moore G, Vennemann T, Carmichael ISE (1998) An empirical model for the solubility of H_2O in magmas to 3 kilobars. Am Mineral 83:36–42

Nakagawa M (1987) Geology of Iwate volcanic group, northeastern Japan. J Mineral Petrol Econ Geol 82:132–150 (in Japanese with English abstract)

Nielsen CH, Sigurdsson H (1981) Quantitative methods for electron microprobe analysis of sodium in natural and synthetic glasses. Am Mineral 66:547–552

Onuma K (1962) Petrography and petrochemistry of the rocks from Iwate volcano, northeastern Japan. J Mineral Petrol Econ Geol 47:192–204

Panjasawatwong Y, Danyushevsky LV, Crawford AJ, Harris KL (1995) An experimental study of the effect of melt composition on plagioclase-melt equilibria at 5 and 10 kbar: inplications for the origin of magmatic high-An plagioclase. Contrib Mineral Petrol 118:420–432

Roggensack K, Hervig RL, Mcknight SB, Williams SN (1997) Explosive basaltic volcanism from Cerro Negro Volcano: Influence of volatiles on eruptive style. Science 277:1639–1642

Sato H (1989) Fe-Mg partitioning between plagioclase and liquid in basalts of Hole 504B, OPD LEG 111: a study of melting at 1 atm. Proc ODP Sci Res 111:17–26

Sato H, Nakada S, Fujii T, Nakamura M, Kamata S-K (1999) Groundmass pargasite in the 1991–1995 dacite of Unzen volcano: phase stability experiments and volcanological implications. J Volc Geotherm Res 89:197–212

Scaillet B, Evans BW (1999) The 15 June 1991 eruption of Mount Pinatubo. É. Phase equilibria and pre-eruption P-T-fO_2-fH_2O conditions of the dacite magma. J Petrol 40:381–411

Shibata T, Nakamura E (1997) Across-arc variations of isotopes and trace element compositions from Quaternary basaltic volcanic rocks in northeastern Japan: Implications for interaction between subducted oceanic slab and mantle wedge. J Geophys Res 102:8051–8064

Singer BS, Pearce TH, Kolisnik AM, Myers JD (1993) Plagioclase zoning in mid-Pleistocene lavas from the Seguam volcanic center, central Aleutian arc, Alaska. Am Mineral 78:143–157

Sisson TW, Bronto S (1998) Evidence for pressure-release melting beneath magmatic arcs from basalt at Galunggung, Indonesia. Nature 391:883–886

Sisson TW, Grove TL (1993a) Experimental investigations of the role of H_2O in calc-alkaline differentiation and subduction zone magmatism. Contrib Mineral Petrol 113:143–166

Sisson TW, Grove TL (1993b) Temperatures and H_2O contents of low-MgO high-alumina basalts. Contrib Mineral Petrol 113:167–184

Sisson TW, Layne GD (1993) H_2O in basalt and basaltic andesite glass inclusions from four subduction-related volcanoes. Earth Planet Sci Lett 117:619–635

Sobolev AV, Chaussidon M (1996) H_2O concentrations in primary melts supra-subduction zones and mid-ocean ridges: Implications for H_2O storage and recycling in the mantle. Earth Planet Sci Lett 137:45–55

Sugawara T (1999) Experimental techniques to minimize Fe and Na losses in one atmosphere gas mixing furnace. J Mineral, Petrol Econo Geol 94:425–441

Sugawara T (2001) Ferric iron partitioning between plagioclase and silicate liquid: thermodynamics and petrological applications. Contrib Mineral Petrol 141:659–686

Tatsumi Y (1989) Migration of fluid phases and genesis of basalt magmas in subduction zones. J Geophys Res 94:4697–4707

Tsukui M, Hoshino K (2002) Magmatic differentiation of Hachijo-Nishiyama volcano, Izu Islands, Japan. Bull Volc Soc Japan 47:57–72 (in Japanese with English abstract)